ELSEVIER

Marine Micropaleontology 27 (1996) 313–326

MARINE MICROPALEONTOLOGY

Mid-Pliocene warmth: stronger greenhouse and stronger conveyor

M.E. Raymo [a], B. Grant [a], M. Horowitz [a], G.H. Rau [b,c]

[a] *Department of Earth, Atmospheric, and Planetary Sciences Massachusetts Institute of Technology, Cambridge MA 02139, USA*

[b] *University of California, Institute of Marine Sciences, Santa Cruz, CA 95064, USA*

[c] *Global Climate Research Division, Lawrence Livermore National Laboratory, Livermore, CA 9 4551, USA*

Received 1 October 1994; accepted 1 May 1995

Abstract

Three million years ago, prior to the onset of northern hemisphere glaciation, global mean temperatures may have been as much as 3.5°C warmer than at present. We present evidence, based on the carbon isotopic composition of marine organic matter, that atmospheric CO_2 levels at this time were on average only about 35% higher than the preindustrial value of 280 ppm. We also present carbon isotopic evidence for stronger thermohaline circulation in the Atlantic Ocean during the warmest intervals and propose that the North Atlantic "conveyor belt" may act as a positive feedback to global warming by enhancing sea ice retreat and decreasing high latitude albedo. Based on our results, it seems unlikely that the mid Pliocene warm period was a doubled CO_2 world.

1. Introduction

Global deforestation and the combustion of fossil fuels has resulted in a pronounced and rapid increase in the concentration of atmospheric CO_2 over the last 150 years. While the preindustrial level (PIL) of CO_2 hovered around 280 ppm for thousands of years, the present day level is about 355 ppm ($\sim$25% increase) and is predicted to double sometime in the next century (Houghton et al., 1990). Because CO_2 is a "greenhouse" gas, a major concern is whether this increase will result in global warming (Houghton et al., 1990) and, if so, what the magnitude of that warming will be. One approach to this problem is to identify times in the geologic past with "doubled" CO_2 levels and see how climate was different. Of course one would have to be certain that other climatic influences, in particular, the tectonic positioning of plates and orography (land and ice) were properly taken into consideration. Even then, a comparison could be misleading since any geologic interval of more than a few thousand years would presumably reflect an equilibrium state while future warming, if any, will reflect a non-equilibrium perturbation of the climate system (Crowley, 1990). Unfortunately, direct measurements of atmospheric CO_2 only go back about 200,000 years and at no time during this interval was the atmospheric level more than 10% above Holocene levels.

A second approach to identifying greenhouse "analogs" in the geologic record is to compare the distribution of surface temperatures in the past to that predicted by $2\times CO_2$ general circulation model (GCM) experiments. Using this approach Budyko et al. (1987) and later Crowley (1991) pointed out that the magnitude of high latitude warming estimated for the mid Pliocene was similar to that observed in $2\times CO_2$ GCM runs and, therefore, the middle Pliocene might have been a period of significantly higher ($2\times$) atmospheric CO_2 levels. However, other investigators countered that Pliocene warmth, in particular at high

SSDI 0377-8398(95)00048-8

latitudes, could be due to greater ocean heat transport (e.g. Rind and Chandler, 1991) and that there was no need to invoke higher CO_2 levels. These ideas stimulated many detailed investigations of the middle Pliocene (this issue and references therein) in an effort to understand the origin of climate warmth (and variability) at this time. In this paper we present an investigation of Pliocene ocean–atmosphere CO_2 levels based on the $\delta^{13}C$ of marine organic matter. We also investigate the strength of thermohaline circulation in the Atlantic using carbon isotope ratios preserved in the shells of benthic foraminifera. We find that global warming appears to have occurred in association with only slightly higher atmospheric CO_2 levels. We also present evidence suggesting the North Atlantic circulation "conveyor" was more vigorous during periods of maximum warmth.

The mid-Pliocene, around three million years ago, was the most recent extended period in the past significantly warmer than today. Arctic sea ice was probably substantially reduced (Carter et al., 1986; Repenning et al., 1987; Brigham-Grette and Carter, 1992; Cronin et al., 1993); high-latitude surface air temperatures may have been up to 10°C warmer than today (Budyko and Izrael, 1987); mid-latitude sea surface temperatures (SSTs) were possibly warmer by as much as 3–4°C (Cronin, 1991; Dowsett et al., 1992, 1994); and finally, sea level is estimated to have been ~25 m higher (Dowsett and Cronin, 1990) probably due to partial deglaciation of East Antarctica (Barrett et al., 1992). The two hypotheses offered to explain global warming at this time, doubled atmospheric CO_2 levels and increased poleward ocean heat transport, were evaluated by Dowsett et al. (1992) who estimated low-latitude sea-surface temperatures (SSTs) in the Pliocene; a doubling of atmospheric CO_2 is predicted to cause a 2–3°C warming of equatorial SSTs while increased ocean heat transports would cause low-latitude SSTs to warm by only 1°C (Rind and Chandler, 1991). They concluded that tropical SSTs increased only slightly and, therefore, that greater ocean heat transport was instrumental in increasing high-latitude temperatures. Here, two more tests of the above hypotheses are presented: (1) paleo-pCO_2 estimates based on the $\delta^{13}C$ of marine organic matter, and (2) estimates of North Atlantic Deep Water (NADW) production based on reconstruction of inorganic $\delta^{13}C$ gradients in the Pliocene ocean.

2. Paleo-pCO_2 estimates

A number of experimental, theoretical, and field studies have shown that $\delta^{13}C$ in marine plankton, including suspended and sedimentary particulate organic matter (POM), varies inversely as a function

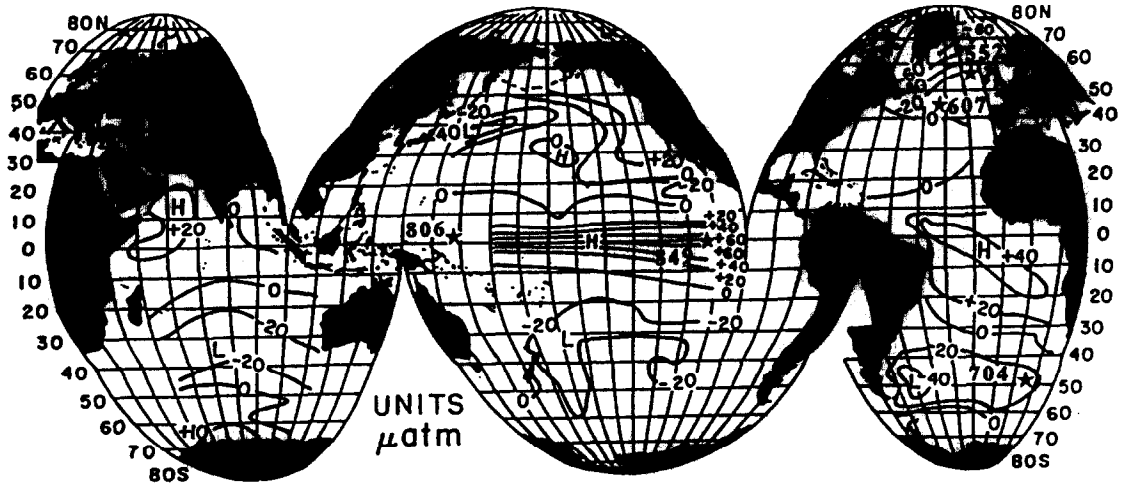

Fig. 1. Map of air–sea CO_2 difference based on results of numerous oceanographic expeditions. Positive values reflect excess partial pressure of CO_2 in surface waters (in μatm). Site 806 as well as four sites used to reconstruct deep water gradients in $\delta^{13}C$ of ΣCO_2 are shown (figure modified from Broecker and Peng, 1993).

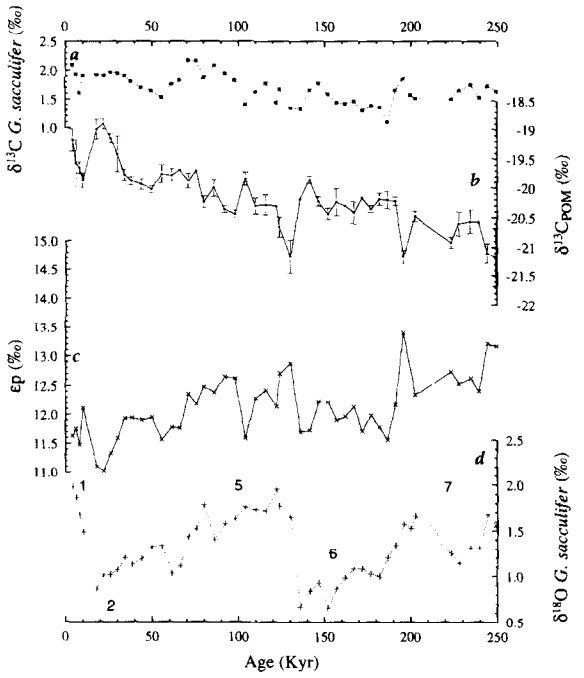

Fig. 2. Estimates of late Pleistocene ocean pCO_2 levels at Site 806 are based on the following data: (a) $\delta^{13}C$ of *G. sacculifer* is used to constrain surface water $\delta^{13}C_{CO2(aq)}$ as per Eqs. 3 and 4 in text; (b) mean $\delta^{13}C_{POM}$ of sediment at each level where error bars represent the standard deviation of replicates from that sample, typically three; (c) calculation of ϵp as per Eq. 2; (d) planktic $\delta^{18}O$ stratigraphy with isotopic stages identified.

of ambient $CO_{2(aq)}$ concentration, $[CO_{2(aq)}]$ (Mizutani and Wada, 1982; Arthur et al., 1985; McCabe, 1985; Popp et al., 1989; Rau et al., 1989, 1991, 1992; Jasper and Hayes, 1990; Francois et al., 1993). Surface ocean $[CO_{2(aq)}]$ and pCO_2 are interrelated via a temperature and salinity dependent solubility factor, α, such that ocean $pCO_2 = [CO_{2(aq)}]/\alpha$. By measuring the $\delta^{13}C$ of marine organic matter preserved in deep sea sediments and using the above relationships, a number of studies have attempted to reconstruct ocean pCO_2 levels in the past (Freeman and Hayes, 1992; Stott, 1992; Jasper et al., 1994). In particular, many low-latitude sediment core $\delta^{13}C_{POM}$ records show a 1–2‰ decrease across the last glacial–interglacial (G–I) transition corresponding to a mean surface ocean pCO_2 increase of about 80 μatms, as confirmed from ice cores (e.g. Rau et al., 1991; Rau, 1994; Muller et al., 1994; this paper). Here we apply this proxy technique to the problem of Pliocene pCO_2 levels by examining marine POM $\delta^{13}C$ at ODP Site 806 in the western equatorial Pacific (0°N, 159°E, 2520 meters below seafloor, mbsf).

On average, the surface ocean pCO_2 is in thermodynamic equilibrium with the atmosphere, however, areas of air/sea disequilibrium arise when seasonal upwelling or productivity results in CO_2 supersaturation or undersaturation, respectively (Fig. 1; Tans et al., 1990; Pedersen et al., 1991; Inoue and Sugimura, 1992; Rau et al., 1992; Takahashi et al., 1993). In applying the paleo-pCO_2 method to the estimation of past atmospheric CO_2 levels, one would ideally like a site where SSTs were well-known (so that CO_2 solubility, α, is well constrained) and where approximate equilibrium with the atmosphere was maintained. Site 806 is not in perfect equilibrium with the atmosphere, however, it is located within the "warm pool", a region of exceptionally stable seasonal and G–I SSTs. This region is generally supersaturated by about 20–60 ppm, on average, with respect to atmospheric pCO_2 due to weak equatorial upwelling, although values range from

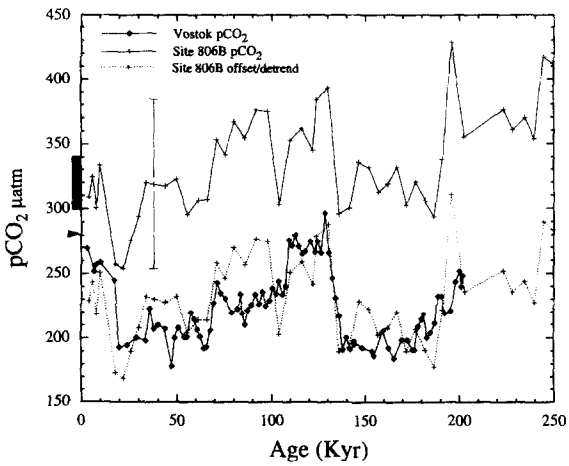

Fig. 3. Estimate of ocean pCO_2 at Site 806 (+) compared to the Vostok CO_2 record (♦). Shaded area on left axis indicates typical range of supersaturation in this region as discussed in text while arrow points to recent preindustrial atmospheric CO_2 level of 280 ppm. Superimposed on Vostok CO_2 record is the 806 record with long term secular trend removed and then shifted downward by a constant value (... + ...). The relatively good correlation between these two records suggests that random errors introduced by regression of ϵp versus $[CO_{2(aq)}]$ in the modern ocean are not as large as ±65 ppm (or ±2 μmole/kg), the error bar shown on figure.

Table 1

ODP/DSDP sample ID	Comp. depth (m)	Age (kyr)	$\delta^{13}C_{POM}$ (‰)	C/N	$\delta^{13}C_{DIC}$ (‰)[a]	SST_{mean} (°C)	ϵp (‰)	pCO_2 (μatm)
1-1, 9 cm	0.09	4.0	−19.2	6.0	1.39	29.5	11.6	309
1-1, 19 cm	0.19	6.0	−19.6	5.9	1.23	29.3	11.9	325
1-1, 29 cm	0.28	8.0	−19.7	5.7	0.90	28.9	11.6	301
1-1, 39 cm	0.38	10.0	−19.9	6.3	1.21	28.5	12.1	334
1-1, 49 cm	0.47	18.0	−19.0	8.1	1.22	27.3	11.1	258
1-1, 59 cm	0.57	22.0	−18.9	7.0	1.21	27.6	11.0	254
1-1, 69 cm	0.66	26.0	−19.2	7.0	1.26	27.6	11.3	275
1-1, 79 cm	0.75	30.0	−19.4	7.0	1.25	27.7	11.6	294
1-1, 89 cm	0.85	34.0	−19.8	7.7	1.21	28.0	11.9	320
1-1, 99 cm	0.94	38.0	−19.9	7.3	1.11	27.8	11.9	319
1-1, 109 cm	1.04	43.8	−19.9	6.9	1.0	28.0	11.9	317
1-1, 119 cm	1.13	49.7	−20.0	6.8	0.95	28.2	12.0	323
1-1, 129 cm	1.22	55.5	−19.8	na	0.83	28.2	11.6	296
1-1, 139 cm	1.32	61.4	−19.8	7.2	1.06	27.6	11.8	306
1-1, 148 cm	1.40	66.0	−19.7	7.3	1.13	27.8	11.8	307
1-2, 9 cm	1.51	71.0	−19.9	6.3	1.48	28.4	12.4	353
1-2, 19 cm	1.60	75.5	−19.7	6.9	1.47	28.6	12.2	342
1-2, 29 cm	1.70	80.0	−20.2	5.9	1.17	29.1	12.5	367
1-2, 39 cm	1.79	86.0	−20.0	6.6	1.38	28.4	12.4	354
1-2, 49 cm	1.88	92.0	−20.4	6.9	1.25	28.7	12.7	376
1-2, 59 cm	1.98	98.0	−20.4	6.8	1.13	28.8	12.6	375
1-2, 69 cm	2.07	104.0	−19.9	5.7	0.70	29.1	11.6	303
1-2, 79 cm	2.17	110.0	−20.3	6.3	0.93	29.0	12.3	353
1-2, 89 cm	2.26	116.0	−20.3	6.7	1.08	29.0	12.4	362
1-2, 99 cm	2.36	122.0	−20.3	7.0	0.74	29.4	12.1	345
1-2, 109 cm	2.44	124.0	−20.7	5.1	0.97	29.1	12.7	383
1-2, 119 cm	2.54	130.3	−21.2	6.1	0.64	28.9	12.9	393
1-2, 129 cm	2.64	136.0	−20.2	7.8	0.62	26.9	11.7	296
1-2, 139 cm	2.73	141.6	−19.9	7.6	0.96	27.3	11.7	300
1-2, 146 cm	2.82	146.6	−20.2	na	1.07	27.5	12.2	336
1-3, 9 cm	2.92	152.1	−20.4	7.1	0.89	26.9	12.2	332
1-3, 19 cm	3.01	157.1	−20.2	7.7	0.74	27.3	11.9	313
1-3, 29 cm	3.11	162.1	−20.3	7.5	0.72	27.5	12.0	319
1-3, 39 cm	3.20	167.0	−20.4	7.4	0.76	27.8	12.1	332
1-3, 49 cm	3.30	172.0	−20.2	7.4	0.60	27.7	11.7	303
1-3, 59 cm	3.39	177.0	−20.4	7.8	0.68	27.6	12.0	321
1-3, 69 cm	3.49	182.0	−20.2	7.3	0.65	27.6	11.8	306
1-3, 79 cm	3.58	186.6	−20.2	8.1	0.39	28.0	11.6	294
1-3, 89 cm	3.67	191.2	−20.2	na	0.96	28.3	12.2	339
1-3, 99 cm	3.77	195.8	−21.2	7.8	1.16	28.7	13.4	429
1-3, 108 *cm*[b]	3.85	199.9	−22.9	7.1	0.87	28.6	14.8	529
1-3, 114 cm	3.91	202.7	−20.5	6.0	0.81	28.9	12.3	355
1-4, 9 cm	4.33	223.4	−20.9	6.8	0.80	28.1	12.7	376
1-4, 19 cm	4.43	228.0	−20.6	7.2	0.95	27.9	12.5	360
1-4, 29 cm	4.52	234.6	−20.6	6.8	1.05	28.2	12.6	370
1-4, 39 cm	4.62	239.5	−20.6	7.1	0.83	28.2	12.4	354
1-4, 49 cm	4.71	244.4	−21.1	5.6	1.02	28.9	13.2	417
1-4, 59 cm	4.80	249.3	−21.2	5.3	0.94	28.7	13.2	412
8-2, 83 cm	65.89	2909.4	−21.4	6.7	0.79	28.8	13.2	419
8-2, 93 cm	65.99	2912.0	−21.1	6.4	1.05	28.8	13.2	415
8-3, 133 cm	67.89	2966.2	−21.3	9.4	1.26	29.0	13.6	446
8-4, 23 cm	68.29	2977.5	−21.1	7.6	1.14	28.1	13.2	410
8-4, 63 cm	68.69	2988.0	−21.1	7.7	0.81	28.6	13.0	396
8-4, 93 cm	68.99	2997.4	−20.8	9.9	1.05	28.0	12.8	380

ODP/DSDP sample ID	Comp. depth (m)	Age (kyr)	$\delta^{13}C_{POM}$ (‰)	C/N	$\delta^{13}C_{DIC}$ (‰)[a]	SST_{mean} (°C)	ϵp (‰)	pCO_2 (μatm)
8-5, 3 cm	69.59	3014.4	−20.5	9.4	1.44	28.7	13.0	400
8-5, 23 cm	69.79	3020.1	−20.9	9.6	1.66	27.7	13.5	425
8-5, 43 cm	69.99	3025.7	−21.0	7.6	1.01	29.1	13.1	409
8-5, 103 cm	70.59	3042.7	−20.7	10.0	1.10	29.5	12.9	401
8-6, 13 cm	71.19	3059.8	−20.4	7.9	1.10	29.1	12.5	369
8-6, 103 cm	72.09	3085.3	−21.3	9.1	0.86	28.7	13.2	415
8-6, 133 cm	72.39	3093.8	−21.0	10.9	1.25	28.7	13.3	419
8-6, 143 cm	72.49	3096.6	−21.0	10.2	1.25	28.2	13.2	409
8-7, 13 cm	72.69	3102.3	−21.2	8.7	0.98	28.2	13.2	410
8-7, 53 cm	73.04	3112.2	−21.1	8.8	1.24	29.1	13.5	436
9-1, 73 cm	73.64	3129.3	−21.1	8.7	1.69	29.0	13.9	465
9-1, 93 cm	73.81	3134.2	−21.3	8.3	1.52	28.9	13.9	467
9-2, 53 cm	74.78	3161.6	−21.0	8.3	1.48	28.9	13.5	440
9-2, 93 cm	75.18	3173.0	−21.0	9.5	1.57	28.1	13.5	432
9-3, 14 cm	75.89	3192.8	−21.1	9.4	1.20	28.5	13.3	419
9-3, 33 cm	76.08	3198.5	−20.8	10.8	1.37	28.5	13.2	413
9-3, 93 cm	76.68	3215.5	−21.3	10.8	0.91	27.8	13.2	406
9-3, 133 cm	77.08	3226.9	−21.1	10.2	0.98	27.9	13.1	402
9-4, 13 cm	77.41	3236.1	−21.4	9.5	1.10	28.4	13.6	437
9-4, 23 cm	77.53	3239.7	−21.0	10.1	1.30	28.4	13.3	419
9-4, 33 cm	77.66	3243.3	−21.6	9.9	1.07	28.4	13.7	448
9-4, 73 cm	78.17	3257.7	−21.5	9.7	0.76	28.7	13.3	420
9-4, 93 cm	78.42	3264.9	−21.4	8.7	0.87	28.3	13.3	416
9-5, 3 cm	79.19	3286.6	−21.1	9.8	0.90	28.6	13.1	405
9-5, 53 cm	79.82	3304.6	−21.4	9.6	1.15	27.9	13.6	433
9-6, 33 cm	81.24	3344.9	−21.4	10.6	1.35	28.4	13.8	457
9-6, 63 cm	81.54	3353.4	−21.2	10.7	1.31	29.2	13.6	450
9-7, 13 cm	82.54	3381.7	−21.5	10.1	1.39	29.1	14.0	475

[a] $\delta^{13}C_{DIC}$ values determined from $\delta^{13}C$ of *G. sacculifer* minus 0.7‰ [data from Schmidt et al. (1993) and unpubl. data of E. Jansen]. Composite depths determined from Berger et al. (1993) and Jansen et al. (1993). All age estimates are calibrated to time scale of Shackleton et al. (1990).
[b] This sample not included in figures as replicate analyses show consistently negative isotopic values giving anomalously high pCO_2 estimates.

slightly undersaturated to oversaturated by +80 ppm during El Niño climatological extremes (Inoue and Sugimura, 1992). We discuss potential biases from these factors below.

At Site 806, a 250 kyr late Pleistocene record was generated for comparison with the Vostok ice core CO_2 record (Barnola et al., 1987) and to provide a base line against which the Pliocene estimates could be compared (Fig. 2 and Fig. 3). In the mid Pliocene interval between 2.9 and 3.3 Ma (time scale of Shackleton et al., 1990, which is approximately equivalent to 2.75–3.15 Ma in the time scale of Berggren et al., 1985), samples representing both warm and cold climate extremes (as inferred from $\delta^{18}O$) were analyzed. Approximately 100 mg samples of bulk sediment were acidified with excess 1 *N* HCl and rinsed in distilled water. After drying, the remaining residue was transferred to a tin cup for combustion in NA1500 Carlo Erba Elemental Analyzer. The evolved CO_2 gas is carried in a helium stream to a VG Prism III mass spectrometer where the $\delta^{13}C$ relative to PDB is determined (Table 1). OC yield and C/N ratios are also determined for each sample by integration of peak areas for C and N. All samples were prepared, acidified, and measured in triplicate or quadruplicate at MIT and average standard deviation for standards (benzoic acid) and sample replicates is ±0.10‰ and ±0.18‰ respectively. In other words, the 0.18‰ includes variability associated with sample prep procedures.

Assuming that the measured isotopic variations are a true reflection of past isotopic variations within the plankton communities (see next paragraph), estimates of past $[CO_{2(aq)}]$ were determined using the following equation (Freeman and Hayes, 1992):

$$[CO_{2(aq)}] = 1.84(\epsilon p) - 13.5 \quad (1)$$

where

$$\epsilon p \approx \delta^{13}C_{CO_{2(aq)}} - \delta^{13}C_{plant}$$
$$= ((\delta^{13}C_{CO_{2(aq)}} + 1000)/$$
$$(\delta^{13}C_{plant} + 1000) - 1)(1000) \quad (2)$$

This equation is empirically derived from modern oceanographic data, and has a $[CO_{2(aq)}]$ estimation error of about 2 μmole/kg (Rau, 1994), or a global ocean pCO_2 estimation error averaging ±65 ppm but ranging from ±46 to ±80 ppm over a temperature range of 12–30°C. (Note that much of this modern oceanographic data uses indirect or non-contemporaneous estimates of $[CO_{2(aq)}]$ which may artificially increase the error associated with subsequent empirical regressions.) In the open ocean environment $\delta^{13}C_{plant}$ is assumed to be represented by $\delta^{13}C_{POM}$, and $\delta^{13}C_{CO2(aq)}$ is determined from planktic foraminifera $\delta^{13}C$ estimates of dissolved inorganic carbon (DIC), corrected for the effects of changing SST on the $CO_{2(aq)}$ equilibrium isotopic value using the following equations (Jasper et al., 1994):

$$\delta^{13}C_{CO_{2(aq)}} =$$
$$((\delta^{13}C_{DIC(foram)} + 1000)/$$
$$(\epsilon_{m/d} + 1000)) - 1)(1000) \quad (3)$$

where

$$\epsilon_{m/d} = -14.07$$
$$+ (7050/SST) \text{ and SST is in Kelvin} \quad (4)$$

Holocene coretop foraminifera $\delta^{13}C$ values were calibrated to modern measurements of the $\delta^{13}C$ of total inorganic carbon of surface water at nearby GEOSECS station 246 (Kroopnick, 1985).

Since bulk sedimentary organic matter (OM) is analyzed, the presence of isotopically distinct terrestrial OM could mask the $\delta^{13}C$ of the marine OM. Such a bias would be sensitive both to the type of terrestrial OM input (e.g. C3 or C4 plants) and the amount of such contamination. Few quantitative estimates of such input to the region studied here have been made, although Prahl et al. (1989) estimate 20% aeolian derived terrestrial OM at MANOP Site C in the eastern equatorial Pacific (139°W). By contrast, at a site further to the east (134°W), Emerson et al. (1987) estimate that the bulk of the sedimentary OM was of marine origin. Site 806 is located far from any direct source of terrestrial matter input, on an oceanic plateau, and would only be susceptible to long-range aeolian transport of OM. Although this site is today located in a region of prevailing easterly trade winds, modern and sedimentologic studies indicate that the major source area for dust supplied to this region is Asia. This dust is carried by prevailing westerlies to lower latitudes where it is entrained by easterly trade winds, eventually being deposited in the equatorial regions (Krissek and Janecek, 1993). While a secondary local source of aeolian material may exist near the Ontong–Java Plateau (Krissek and Janecek, 1993), the bulk of aeolian-transported material appears to derive from the arid regions of central Asia. It seems unlikely that such a source region could provide a significant source of OM given the sparse vegetative cover typically found in arid regions, however, the possibility remains and needs to be tested.

At Site 806, C/N ratios for Pleistocene samples fall within a typical marine OM range of ~6–8 (Bordowskiy, 1965; Fig. 4; Table 1). By contrast, terrestrial C/N ratios are typically greater than 20 (Hedges and Parker, 1976). Hydrogen index values at Site 806 are also indicative of marine OM (Stax and Stein, 1993). Site 806 does show a trend to higher C/N in the older Pliocene samples (range from 7 to 11; Fig. 4). If this trend was due to more terrestrial OM contamination in the Pliocene, then the 806 samples would be overestimating pCO_2 at that time. Detailed dust studies have not yet been extended into the Pliocene, however, the Pleistocene interval at this site shows a subtle increase in dust flux toward the present (L.A. Krissek, unpubl. data, pers. commun., 1995) suggesting that if terrestrial contamination was occurring it is increasing over the Pleistocene, opposite of the trend in the C/N ratios.

The possibility of small amounts of terrestrial OM contaminating our samples is a concern. A 10% contribution of C3 terrestrial organic matter (~ −27‰) would bias the $\delta^{13}C_{POM}$ value (and subsequent ϵp) by about 0.6‰, changing the $[CO_{2(aq)}]$ and pCO_2 estimates by about 15% (Eq. 1). Such a bias would presumably be greatest at times of greatest aeolian input at our sites. Analysis of specific biomarkers may help constrain this potential error by identifying whether significant terrestrial OM exists in these samples. Likewise, one could measure biomarker $\delta^{13}C$ values to esti-

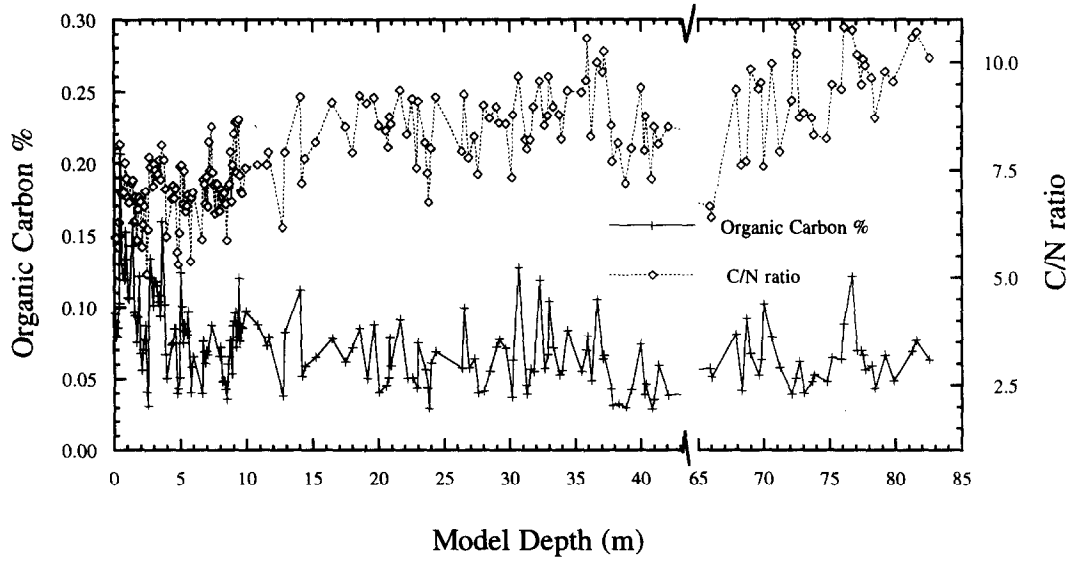

Fig. 4. Long term trends in %organic carbon and C/N elemental ratios at Site 806.

mate the $[CO_{2(aq)}]$ change from the Pliocene to the present. However, unlike for $\delta^{13}C_{POM}$ data, there appears to be no regionally applicable regression relation between biomarker ϵp and $[CO_{2(aq)}]$ (e.g. Jasper et al., 1994). The fact that *E. huxleyi*, the primary source of the alkenones used in late Pleistocene biomarker studies, did not exist prior to stage 8 (~ 300 kyr B.P.; Thierstein et al., 1977) would also need to be considered.

Another uncertainty in our results is that $\delta^{13}C_{POM}$ may be modified from the original surface water photosynthate by isotopically selective metabolism and diagenesis, either in the water column or in the sediment. For instance, the preferential preservation of refractory components with distinctive isotopic signatures could bias $\delta^{13}C_{POM}$. At the moment this error remains essentially unquantifiable. During diagenesis, one might also expect the C/N ratio to increase downcore as N-enriched OM components are preferentially degraded (e.g. Muller, 1977). At site 806, C/N does increase downcore, as pointed out above, while %OM decreases; however, the increase in C/N ratios happens deeper in the core than the decrease in %OM (Fig. 4). This long term trend varies in the opposite sense of the late Pleistocene G–I trend where glacial intervals have higher %OM and higher C/N ratios. If downcore diagenesis overprints the 806 $\delta^{13}C_{POM}$ record then this imprint most likely occurs in the first 200,000 years of burial. This is the interval over which %OM goes from about 0.10 to 0.15 in the last G–I cycle, to a long term Plio-Pleistocene average of about 0.04 to 0.08% (Fig. 4). Over the last 200 kyr, $\delta^{13}C_{POM}$ values also exhibit a secular trend from about $-21.0‰$ at depth to $-19.0‰$ near the core top. Post-burial degradation may explain the decrease in %OM and the trend in $\delta^{13}C_{POM}$ which is approximately the same direction and magnitude as that observed by McArthur et al. (1992) in turbidites on the Madeira Abyssal Plain. They attributed their trend to diagenesis. Note that this would imply that isotopically enriched OM is preferentially degrading downcore. Another possibility is that preferential degradation of marine OM over terrestrial would lead to decreased $\delta^{13}C_{POM}$ downcore, however, this possibility is not supported by C/N ratios which show an increase much deeper in the core (e.g. no secular trend over the interval of decreasing %OM). Recent studies of OM preservation have focused on the role played by mineral surface areas in adsorbing and protecting labile OM from degradation (e.g. Mayer, 1994; Keil et al., 1994). If this mechanism for OM preservation is important then it is more likely that a representative distribution of POM, rather than only the most refractory material, is preserved in deep sea sediments.

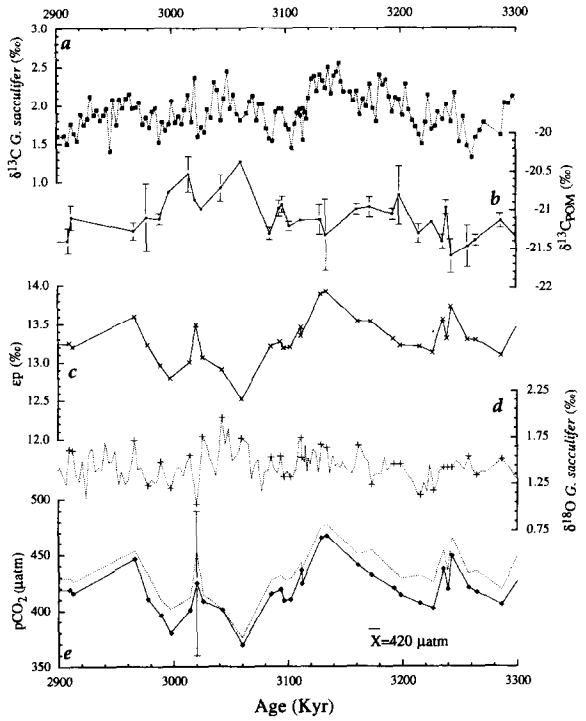

Fig. 5. Ocean pCO_2 estimates for middle Pliocene interval at Site 806 (e) based on $\delta^{13}C$ of *G. sacculifer* (a) and $\delta^{13}C_{POM}$ (b). ϵp shown in (c) with planktic $\delta^{18}O$ record in (d). Note that crosses (+) on this record indicate which samples were analyzed for $\delta^{13}C_{POM}$. The error bars are the same as described in Figs. 2 and 3, while the dashed line indicates ocean pCO_2 obtained when SST is held constant at modern levels.

Here we present the $\delta^{13}C_{POM}$ data at face value and caution the reader to keep possible biases associated with contamination and diagenesis in mind. This source of error is not reflected in the error bars in Fig. 3 and Fig. 5e which are associated with the regression of $[CO_{2(aq)}]$ vs. $\delta^{13}C_{POM}$. After estimating $[CO_{2(aq)}]$ from the isotopic data we determine pCO_2 by dividing $[CO_{2(aq)}]$ by the solubility constant, α, which is estimated from SST using the equation of Weiss (1974). Salinity, a second order influence on solubility, is assumed to be 35‰. Past changes in SST were estimated by scaling the $\delta^{18}O$ change between stage 1 and 2 to the glacial–interglacial change in mean SST estimated by CLIMAP (1981). This method assumes that the amount of SST change per unit of ice volume change has remained constant, however, since seasonal SST variability ($\sim$1°C) and G–I SST variability ($\sim$2.5°C) is so small, errors associated with this assumption are probably minimal. There is no evidence that SST was significantly higher in the middle Pliocene, possibly because cloud cover and/or evaporation acts as a buffer in this region preventing temperatures from increasing above 30°C (Newell and Hsiung, 1984). It has been suggested that SSTs at Site 806 might have been 2–3°C colder at 3.0 Ma (Jansen et al., 1993) and, if true, would imply that we have underestimated Pliocene CO_2 solubilities and thus overestimated Pliocene pCO_2 (Fig. 5). A 1.5°C estimation error in SST translates to an $\sim$25 ppm error in estimated atmospheric pCO_2 (this includes the error in estimating $\delta^{13}C_{CO2(aq)}$).

Converting the late Pleistocene $\delta^{13}C_{POM}$ data in Fig. 2 to ocean pCO_2 produces a record (Fig. 3, top curve) which shows some remarkable similarities to the ice core pCO_2 record. Both records have been adjusted to a common SPECMAP chronology (Martinson et al., 1987) using the planktic $\delta^{18}O$ record from 806 and the $\delta^{18}O$ of trapped O_2 in the Vostok ice core (Sowers et al., 1993). The estimated Holocene ocean pCO_2 values at site 806 (between 300 and 340 ppm; Fig. 3) fall within the range of moderately supersaturated values observed in this region today (Keeling, 1968; Inoue and Sugimura, 1992). In addition, the G–I terminations in both 806 and the ice core record are of approximately the same magnitude, about 80–100 ppm. One noticeable difference between the two records is the long-term decrease in ocean pCO_2 observed at site 806. This trend is driven primarily by the increase in $\delta^{13}C_{POM}$ values in the top few meters of the core and could only be an atmospheric signal if the Vostok record increasingly underestimates atmospheric pCO_2 levels downcore, a seemingly unlikely possibility (cf Wilson and Long, 1993). By contrast, if this trend was due to a decrease in upwelling intensity in the western equatorial Pacific over the late Pleistocene then we might expect to see a trend imprinted on other paleoceanographic records such as planktic–benthic $\delta^{13}C$ gradients and benthic foraminifera accumulation rates (Herguera, 1994). No obvious secular trends are observed in these proxies in nearby core ERDC 113P (Herguera, 1994). If this trend is caused by preservational or diagenetic processes then the fact that the stage 7 pCO_2 values are approaching those observed for the Pliocene (Fig. 5) implies that we have

overestimated the long-term decrease in ocean pCO_2 levels over the last three million years.

More than two dozen horizons were analyzed in the middle Pliocene interval between 2.9 and 3.3 Ma (Fig. 5) with samples chosen from both positive and negative extremes of the planktic $\delta^{18}O$ record (crosses on Fig. 5d). The average ocean pCO_2 level over this interval is 420 ppm which, when corrected for observed modern ocean–atmosphere disequilibrium, implies an atmospheric CO_2 level closer to 380 ppm. The highest ocean CO_2 levels estimated are about 465 ppm, or ~425 ppm inferred for the mean global atmosphere. With respect to this estimate, can we rule out any long term change in upwelling or productivity intensity that would bias this result? The relative constancy of planktic–benthic $\delta^{13}C$ gradients over the last 3 Ma at Site 806 (Schmidt et al., 1993; Whitman and Berger, 1993) suggests no major change in the dynamics of upwelling and productivity in the western equatorial Pacific. However, if upwelling were stronger in the late Quaternary, this would act to minimize the apparent change in ocean pCO_2 over the last 3 Ma by increasing Quaternary surface water pCO_2. Since the Holocene samples fall in the observed range of supersaturation today, this would imply that the Pliocene ocean pCO_2 levels were closer to equilibrium with atmospheric CO_2 levels and the percentage drop in atmospheric CO_2 since then was slightly larger.

Lastly, it is useful to point out that, based on sensitivities seen in the modern ocean (Rau et al., 1992; Freeman and Hayes, 1992; Francois et al., 1993; Rau, 1994), about a 4‰ reduction in $\delta^{13}C_{POM}$ would be expected for a doubling of atmospheric CO_2 (all else constant). We see no evidence for such a large change in $\delta^{13}C_{POM}$. In the western Pacific, mid Pliocene pCO_2 values appear to be approximately 30% higher than Holocene values (Fig. 1c and d) when adjusted for regional disequilibrium trends and, if the secular trend in $\delta^{13}C_{POM}$ observed near the top of the core is due to diagenesis, then Pliocene pCO_2 levels may have been equal to or slightly higher than Holocene levels. The results from Site 806 are similar to the trend observed in a much smaller data set from the North Atlantic (Raymo and Rau, 1992, 1993). Based on these observations, it seems unlikely that the Pliocene was a doubled CO_2 world.

3. Thermohaline circulation

Another mechanism proposed to cause warming at high latitudes is to increase the strength of the thermohaline "conveyor belt" which pulls warm surface water northward (Broecker and Denton, 1989; Rind and Chandler, 1991). The formation of relatively warm deep water in the North Atlantic may also transmit warmth to high southern latitudes as it upwells around Antarctica (Broecker and Denton, 1989), although this effect could be partially or fully offset by northward cross-equatorial transport of warm thermocline water (Manabe and Stouffer, 1988). Such a change in ocean heat transport could result in a net warming of global climate (as opposed to a redistribution of heat) if it causes a significant reduction in sea ice cover at high latitudes and, therefore, a decrease in global albedo.

In the modern ocean, GEOSECS (1981) measurements clearly show the path traveled by warm, saline, nutrient-depleted (e.g. high $\delta^{13}C$) North Atlantic Deep Water (NADW). As it moves out of the North Atlantic it becomes progressively cooler, fresher, and more nutrient-enriched as it mixes with recirculated Pacific Ocean water (POW) and Antarctic Bottom Water (AABW; Fig. 6a). Modern oceanographic measurements from four DSDP/ODP sites located on a transect from the North Atlantic to the Pacific clearly show mixing between NADW and POW (Fig. 6a) which results in an ~1.3‰ $\delta^{13}C$ gradient between these sites. Reconstruction of past inorganic $\delta^{13}C$ gradients by measurement of calcitic shells of deep water benthic foraminifera allow us to infer the relative strength of NADW formation in the past (e.g. Curry et al., 1988; Raymo et al., 1990a). Fig. 6b shows a compilation of all benthic (*Cibicidoides*) data from these four sites for the interval from ~3.35 to 2.95 Ma. Minimum $\delta^{18}O$ values ~0.5‰ lighter than Holocene values (~3.2‰) were caused by significant warming of the deep ocean and/or major deglaciation of Antarctica; either change is presumably indicative of warmer high latitude temperatures. Note that $\delta^{18}O$ values heavier than present indicate that cool climate extremes (due to Milankovitch forcing) were colder than today (Raymo, 1994). The primary point emphasized by Fig. 6b is that times similar to the Holocene exhibit an overall Aflantic–Pacific $\delta^{13}C$ gradient of ~1.3‰ similar to that observed in the modern ocean (Fig. 6a) while during warmer periods (more negative $\delta^{18}O$),

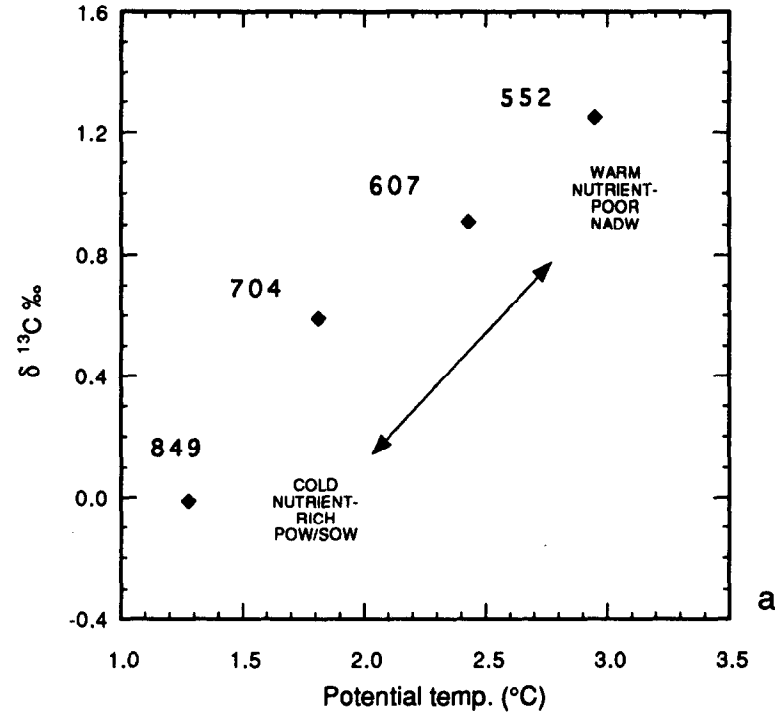
552
607
704
849
WARM NUTRIENT-POOR NADW
COLD NUTRIENT-RICH POW/SOW
δ 13C ‰
Potential temp. (°C)
a

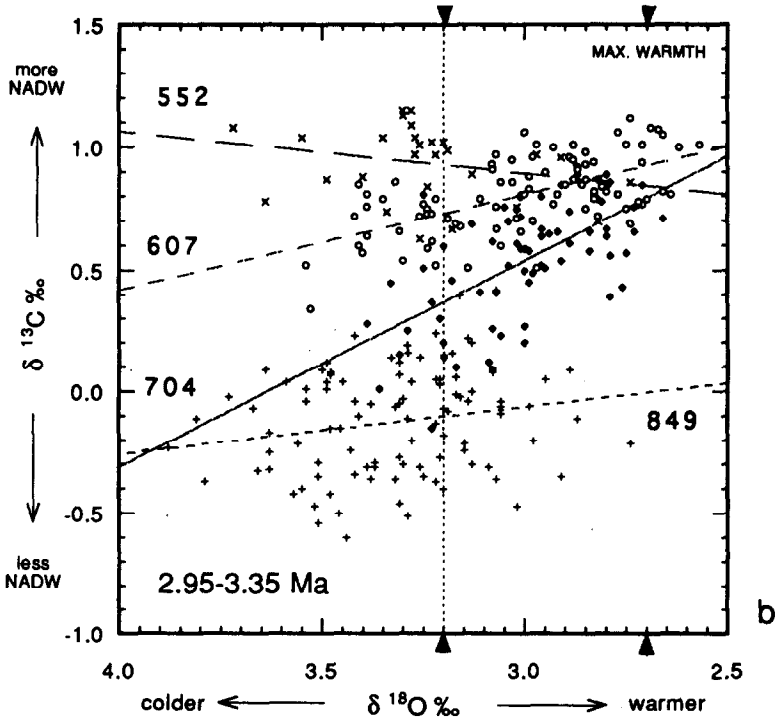
MAX. WARMTH
more NADW
less NADW
552
607
704
849
2.95-3.35 Ma
δ 13C ‰
δ 18O ‰
colder
warmer
b

all the Atlantic sites show very positive, nutrient-depleted $\delta^{13}C$ values. This implies that NADW flooded the deep Atlantic to the exclusion of southern source water (Raymo et al., 1992; Hodell and Venz, 1992). Conversely, colder periods show a weakening of the influence of NADW in the deep Atlantic.

This result is counter to recent ocean GCM experiments which predict that NADW production would weaken as atmospheric CO_2 levels increased (Washington and Meehl, 1989; Mikolajewicz et al., 1990; Manabe et al., 1991; Cubasch et al., 1992; Nakamura et al., 1994). The ocean models attribute the weakening of the NADW conveyor in a warmer world to increased precipitation in the North Atlantic which enhances stratification. However, other factors, including surface water exchange with the Arctic, the intensity of the Icelandic low or polar high, and/or the salinity of imported low latitude surface waters may also influence NADW production (Aagaard and Carmack, 1989; Raymo et al., 1990b; Willebrand, 1993). Likewise, computer models focus on a transient state of global warming which may not be strictly comparable to the longer interval of climate warmth in the Pliocene where deep ocean temperatures have had time to equilibrate with the surface. In any case, with respect to ocean thermohaline circulation, the Pliocene appears to be a period for which the geological record does not match the prediction of climate models.

4. Conclusion

The POM $\delta^{13}C$ data presented above suggest that the middle Pliocene was characterized by atmospheric pCO_2 levels approximately 35% higher than PIL and only slightly higher than today; average CO_2 levels during the middle Pliocene appear to have been about 380 ppm when corrected for ocean–atmosphere disequilibrium. Intervals of peak warmth were up to 45 ppm higher. Our results (which may be an overestimate due to diagenesis) are in general agreement with an estimate of early Pliocene pCO_2 based on the density of stomata in fossil leaves (Van der Burgh et al., 1993) as well as with longer Cenozoic trends estimated from the deep sea carbonate preservation and $\delta^{13}C$ records (Shackleton, 1985; Berger and Spitzy, 1988). Available data suggest that it is unlikely that the mid-Pliocene had atmospheric pCO_2 as high as 560 ppm ($2\times$PIL), but this possibility cannot be conclusively ruled out given uncertainties in our method.

An explanation for the apparently large high latitude warming in the face of a relatively minor CO_2 increase may be that stronger thermohaline circulation acts as a positive feedback enhancing sea ice retreat and, therefore, increasing albedo. Whether warming associated with a modest CO_2 increase resulted in stronger thermohaline circulation or stronger thermohaline circulation (due to some as of yet unknown forcing) caused an increase in atmospheric pCO_2 remains unclear. The important observation is that in the geologic record of the past three million years both processes act to enhance temperatures at high northern latitudes while in ocean–atmosphere GCMs the thermohaline conveyor belt appears to act as a negative feedback.

Acknowledgements

We thank C. Covey, E. Sundquist, and D. Poore for their helpful reviews which greatly improved this paper. We also to thank T. Crowley for his input and support. W. Berger and E. Jansen kindly provided digital files of published 806 data and E. Jansen allowed us to use his unpublished Pliocene $\delta^{13}C$ data. Financial support for this project and the establishment of the lab which produced the bulk of the data was provided by the Exxon Educational Foundation, the Petroleum Research Fund of the American Chemical Society, and

Fig. 6. (a) $\delta^{13}C$ of ΣCO_2 and potential temperature of bottom water at four core locations which define a transect from the region of NADW formation (Site 552 (×), 56°N, 23°W, 2301 mbsf), through the deep Atlantic Ocean (Site 607 (○), 41°N, 33°W, 3427 mbsf; Site 704 (◆), 47°S, 7°E, 2532 mbsf), into the Pacific Ocean (Site 849 (+), 0°N, 111°W, 3851 mbsf). These sites fall on a mixing line between nutrient-depleted deep waters originating in North Atlantic and recirculated nutrient-enriched deep waters from the Pacific and Southern Oceans. (b) $\delta^{13}C$ versus $\delta^{18}O$ of *Cibicidoides* from each of these four sites for interval between 2.95 and 3.35 Ma (includes unpublished 607 data plus data described in Raymo et al., 1992, and Mix et al., 1994). The time scale is consistent with Shackleton et al. (1990). Mean Holocene $\delta^{18}O$ value indicated by vertical dashed line. Periods of peak warmth in the Pliocene have $\delta^{18}O$ values about 2.75‰. Production of NADW increases as the difference between $\delta^{13}C_{552}$ and $\delta^{13}C_{704,607}$ decreases. Lines indicate least squares regression through data from each site.

an NSF NYI award to MER. G.H.R. acknowledges support from the Global Climate Research Division, Lawrence Livermore National Laboratory (Grant SC/95-26), and from NOAA Paleoclimatology Program Grant NA36GP0308.

References

Aagaard, K. and E.C. Carmack, 1989. On the role of sea ice and other fresh water in the Arctic circulation. J. Geophys. Res., 94: 14,485–14,498.

Arthur, M.A., Dean, W.E. and Claypool, G.E., 1985. Anomalous ^{13}C enrichment in modern marine organic carbon. Nature, 315: 216–218.

Barnola, J.M., Raynaud, D., Korotkevich, D.Y.S. and Lorius, C.,1987. Vostok ice core provides 160,000-year record of atmospheric CO_2. Nature, 329: 408–414.

Barrett, P.J., Adams, C.J., McIntosh, W.C., Swisher, C.C. and Wilson, G.S., 1992. Geochronological evidence supporting Antarctic deglaciation three million years ago. Nature, 359: 816–818.

Berger, W.H. and Spitzy, A., 1988. History of atmospheric CO_2: constraints from the deep-sea record. Paleoceanography, 3: 401–411.

Berger, W.H., Bickert, T., Schmidt, H. and Wefer, G., 1993. Quaternary oxygen isotope record of pelagic foraminifers: Site 806, Ontong Java Plateau. Proc. ODP, Sci. Results, 130: 381–395.

Berggren, W.A., Kent, D.V., Flynn, J.J. and Van Couvering, J.A., 1985. Cenozoic geochronology. Geol. Soc. Am. Bull., 96: 1407–1418.

Bordowskiy, O.K., 1965. Accumulation of organic matter in bottom sediments. Mar. Geol., 3: 33–82.

Brigham-Grette, J. and Carter, L.D., 1992. Pliocene marine transgression of northern Alaska: correlations and paleoclimatic interpretations. Arctic, 45: 74–89.

Broecker, W.S. and Denton, G.H., 1989. The role of ocean–atmosphere reorganizations in glacial cycles. Geochim. Cosmochim. Acta, 53: 2465–2501.

Broecker, W.S. and Peng, T., 1993. Greenhouse Puzzles: Part 1. Textbook, 104 pp. (Unpubl.)

Budyko, M. and Izrael, Y.A. (Editors), 1987. Anthropogenic Climate Changes. L. Gidrometeoizdat, Leningrad, 404 pp.

Budyko, M.I., Ronov, A.B. and Yanshin, A.L, 1987. History of the Earth's Atmosphere. Springer, New York, 139 pp.

Carter, L.D., Brigham-Grette, J., Marincovich, L., Pease, V.L. and Hillhouse, J.W., 1986. Late Cenozoic Arctic Ocean sea ice and terrestrial paleoclimate. Geology, 14: 675–678.

CLIMAP, Project Members, 1981. Seasonal reconstructions of the earth's surface at the last glacial maximum. Geol. Soc. Am., Map Chart Ser., MC-36: 1–18.

Cronin, T.M., 1991. Pliocene shallow water paleoceanography of the North Atlantic Ocean based on marine ostracods. Quat. Sci. Rev., 10: 175–188.

Cronin, T.M., Whatley, R.C., Wood, A., Tsukagoshi, A., Ikeya, N., Brouwers, E.M. and Briggs, W.M., 1993. Microfaunal evidence for elevated mid-Pliocene temperatures in the Arctic Ocean. Paleoceanography, 8: 161–173.

Crowley, T.C., 1990. Are there any satisfactory geologic analogs for a future greenhouse warming? J. Clim., 3: 1282–1292.

Crowley, T.C., 1991. Modeling Pliocene warmth. Quat. Sci. Rev., 10: 275–282.

Cubasch, U., Hasselmann, K., Hock, H., Maier-Reimer, E., Mikolajewicz, U., Santer, B.D. and Sausen, R., 1992. Time-dependent greenhouse warming computations with a coupled ocean–atmosphere model. Clim. Dynamics, 8: 55–69.

Curry, W.B., Duplessy, J.C., Labeyrie, L.D., Oppo, D. and Kallel, N., 1988. Quaternary deep-water circulation changes in the distribution of $\delta^{13}C$ of deep water ΣCO_2 between the last glaciation and the Holocene. Paleoceanography, 3: 317–342.

Dowsett H.J. and Cronin, T.M., 1990. High eustatic sea level during the middle Pliocene: Evidence from the southeastern U.S. Atlantic Coastal Plain. Geology, 18: 435–438.

Dowsett, H.J., Cronin, T.M., Poore, R.Z., Thompson, R.S., Whatley, R.C. and Wood, A.M., 1992. Micropaleontological evidence for increased meridional heat transport in the North Atlantic Ocean during the Pliocene. Science, 258: 1133–1135.

Dowsett, H.J., Thompson, R., Barron, J., Cronin, T., Fleming, F., Ishman, S., Poore, R., Willard, D. and Holtz, T., 1994. Joint investigations of the Middle Pliocene climate I: PRISM paleoenvironmental reconstructions. Global Planet. Change, 9: 169–195.

Emerson, S., Stump, C., Grootes, P.M., Stuiver, M., Farwell, G. and Schmidt, F., 1987. Estimates of degradable organic carbon in deep-sea surface sediments from ^{14}C concentrations. Nature, 329: 51–53.

Francois, R., Altabet, M., Goericke, R., McCorkle, D., Brunet, C. and Poisson, A., 1993. Changes in the $\delta^{13}C$ of particulate organic matter suspended in the surface waters across the Subtropical Convergence (STC) in the S.W. Indian Ocean. Global Biogeochem. Cycles, 7: 627–644.

Freeman, K.H. and Hayes, J.M., 1992. Fractionation of carbon isotope by phytoplankton and estimates of ancient CO_2 levels. Global Biogeochem. Cycles, 6: 185–198.

GEOSECS, 1981. Atlantic expedition. Vol. 1 of Hydrographic Data. U.S. Gov. Print. Off., Washington, D.C.

Hedges, J.I. and Parker, P.L., 1976. Land-derived organic matter in surface sediments from the Gulf of Mexico. Geochim. Cosmochim. Acta, 40: 1019–1029.

Herguera, J.C., 1994. Nutrient, mixing, and export indices: a 250 Kyr paleoproductivity record from the western equatorial Pacific. In: R. Zahn et al. (Editors), Carbon Cycling in the Glacial Ocean: Constraints on the Ocean's Role in Global Change. Springer, Berlin, pp. 481–519.

Hodell, D.A. and Venz, K., 1992. Toward a high-resolution stable istopic record of the southern ocean during the Plio-Pleistocene (4.8–0.8 Ma). Antarct. Res. Ser., 56: 265–310.

Houghton, J.T., Jenkins, G.J. and Ephraums J.J. (Editors), 1990. Climate Change: The IPCC Scientific Assessment. Cambridge Univ. Press, Cambridge, 365 pp.

Inoue, H.Y. and Sugimura, Y., 1992. Variations and distributions of CO_2 in and over the equatorial Pacific during the period from the 1896/88 El Niño event to the 1988/89 La Niña event. Tullus, 44B: 1–22.

Jansen, E., Mayer, L., Backman, J., Leckie, M. and Takayama, T., 1993. Evolution of Pliocene climate cyclicity at Hole 806B (5–2 Ma): oxygen isotope record. Proc. ODP, Sci. Results, 130: 349–361.

Jasper, J.P. and Hayes, J.M., 1990. A carbon isotope record of CO_2 levels during the late Quaternary. Nature, 347: 462–464.

Jasper, J., Hayes, J.M., Mix, A. and Prahl, F., 1994. Photosynthetic fractionation of ^{13}C and concentrations of dissolved CO_2 in the central equatorial Pacific during the last 255,000 years. Paleoceanography, 9: 781–798.

Keil, R.G., Montlucon, D., Prahl, F.G. and Hedges, J., 1994. Sorptive preservation of labile organic matter in marine sediments. Nature, 370: 549–552.

Keeling, C.D., 1968. Carbon dioxide in surface ocean waters, 4. Global distribution. J. Geophys. Res., 73: 4543–4553.

Krissek, L.A. and Janecek, T.R., 1993. Eolian deposition on the Ontong Java Plateau since the Oligocene: unmixing a record of multiple dust sources. Proc. ODP, Sci. Res., 130: 471–490.

Kroopnick, P., 1985. The distribution of carbon-13 in the world oceans. Deep-Sea Res., 32: 57–84.

Manabe, S. and Stouffer, R.J., 1988. Two stable equilibria of a coupled ocean–atmosphere model. J. Clim. 1: 841–866.

Manabe, S., Stouffer, R.J., Spelman, M.J. and Bryan, K., 1991. Transient response of a coupled ocean–atmosphere model to gradual changes of atmospheric CO_2. Part I: Annual mean response. J. Climate, 4: 785–818.

Martinson, D., Pisias, N., Hays, J., Imbrie, J., Moore, T. and Shackleton, N., 1987. Age dating and the orbital theory of the ice ages: development of a high-resolution 0 to 300,000-year chronology. Quat. Res., 27: 1–27.

Mayer, L.M., 1994. Surface area control of organic carbon accumulation in continental shelf sediments. Geochim. Cosmochim. Acta, 58: 1271–1284.

McArthur, J.M., Tyson, R.V., Thomson, J. and Mattey, D., 1992. Early diagenesis of marine organic matter: alteration of the carbon isotopic composition. Mar. Geol., 105: 51–61.

McCabe, B., 1985. The dynamics of ^{13}C in several New Zealand lakes. Ph.D., Univ. Waikata, Hamilton, New Zealand.

Mikolajewicz, U., Santer, B.D. and Maier-Reimer, E., 1990. Ocean response to greenhouse warming. Nature, 345: 589–593.

Mix., A, Pisias, N., Rugh, W., Wilson, J., Morey, A. and Hagelberg, T., 1994. Benthic foraminiferal stable isotope record from Site 849, 0–3.2 Ma: local and global climate changes. Proc. ODP, Sci. Results, 138.

Mizutani, H. and Wada, E., 1982. Effect of high atmospheric CO_2 concentration on $\delta^{13}C$ of algae. Origins Life, 12: 377–390.

Muller, P.J., 1977. C/N ratios in Pacific deep-sea sediments: effect of inorganic ammonium and organic nitrogen compounds sorbed by clays. Geochim. Cosmochim. Acta, 41: 765–776.

Muller, P.J., Schneider, R. and Ruhland, J., 1994. Late Quaternary pCO_2 variations in the Angola Current: Evidence from organic carbon $\delta^{13}C$ and alkenone temperatures. In: R. Zahn, M. Kaminski, L.D. Labeyrie and T.F. Pedersen (Editors), Carbon Cycling in the Glacial Ocean: Constraints on the Ocean's Role in Global Change. Springer, Berlin, pp. 343–366.

Nakamura, M., Stone, P. and Marotzke, J., 1994. Destabilization of the thermohaline circulation by atmospheric feedback. J. Climate, 7: 1870–1882.

Newell, R.E. and Hsiung, J., 1984. Sea surface temperature, atmospheric CO_2 and the global energy budget: some comparisons between the past and present. In: N.A. Mörner and W. Karlén (Editors), Climatic Changes on a Yearly to Millennial Basis. Reidel, Dordrecht, pp. 533–561.

Pedersen, T.F., Nelson, B. and Pickering, M., 1991. Timing of late Quaternary productivity pulses in the Panama Basin and implications for atmospheric CO_2. Paleoceanography, 6: 657–677.

Popp, B.N., Takigiku, R. Hayes, J.M., Louda, J.W. and Baker, E.W., 1989. The post-Paleozoic chronology and mechanism of ^{13}C depletion in primary marine organic matter. Am. J. Sci., 289: 436–454.

Prahl, F., Muehlhausen, L. and Lyle, M., 1989. An organic geochemical assessment of oceanographic conditions at MANOP Site C over the past 26,000 years. Paleoceanography, 4: 495–510.

Rau, G.H., 1994. Variations in sedimentary organic $\delta^{13}C$ as a proxy for past changes in ocean and atmospheric [CO2]. In: R. Zahn et al. (Editors), Carbon Cycling in the Glacial Ocean: Constraints on the Ocean's Role in Global Change. Springer, Berlin, pp. 307–322.

Rau, G.H., Takahashi, T. and DesMarais, D.J., 1989. Latitudinal variations in plankton $\delta^{13}C$: implications for CO_2 and productivity in past oceans. Nature, 341: 516–518.

Rau, G.H., Froelich, P.N., Takahashi, T. and Des Marais, D.J., 1991. Does sedimentary organic $\delta^{13}C$ record variations in Quaternary ocean $[CO_2(aq)]$? Paleoceanography, 6: 335–347.

Rau, G.H., Takahashi, T., Des Marais, D.J., Repeta, D.J. and Martin, J.H., 1992. The relationship between organic matter $\delta^{13}C$ and $[CO_{2(aq)}]$ in ocean surface water: data from a JGOFS Site in the Northeast Atlantic Ocean and a model. Geochim. Cosmochim. Acta, 56: 1413–1419.

Raymo, M.E., 1994. The initiation of Northern Hemisphere glaciation. Annu. Rev. Earth Planet. Sci., 22: 353–383.

Raymo, M.E. and Rau, G., 1992. Plio-Pleistocene atmospheric CO_2 levels inferred from POM $\delta^{13}C$ at DSDP Site 607. EOS, Trans. Am. Geophys. Union, 73: 95.

Raymo, M.E. and Rau, G., 1993. Mid-Pliocene warmth: Higher atmospheric CO_2 or stronger ocean heat transports? EOS, Trans. Am. Geophys. Union, 74: 49.

Raymo, M.E., Ruddiman, W.F., Shackleton, N.J. and Oppo, D., 1990a. Evolution of Atlantic–Pacific $\delta^{13}C$ gradients over the last 2.5 m.y. Earth Planet. Sci. Lett., 97: 353–368.

Raymo, M.E., Rind, D. and Ruddiman, W.F., 1990b. Climatic effects of reduced Arctic sea ice limits in the GISS II general circulation model. Paleoceanography, 5: 367–382.

Raymo, M.E., Hodell, D. and Jansen, E., 1992. Response of deep ocean circulation to the initiation of northern hemisphere glaciation (3–2 M.Y.). Paleoceanography, 7: 645–672.

Repenning, C.A., Brouwers, E.M., Carter, L.D., Marincovich, L. and Ager, T.A., 1987. The Beringian ancestry of Phenacomys (Rodentia: Cricetidae) and the beginning of the modern Arctic Ocean borderland biota. U.S. Geol. Surv. Bull., 1687, 29 pp.

Rind, D. and Chandler, M., 1991. Increased ocean heat transport and warmer climate. J. Geophys. Res., 96: 7437–7461.

Schmidt, H., Berger, W., Bickert, T. and Wefer, G., 1993. Quaternary carbon isotope record of benthic foraminifers: Site 806, Ontong Java Plateau. Proc. ODP, Sci. Results, 130: 397–409.

Shackleton, N.J., 1985. Ocean carbon isotope constraints on oxygen and carbon dioxide in the Cenozoic atmosphere. In: E. Sundquist and W. Broecker (Editors), The Carbon Cycle and Atmospheric CO_2: Natural Variations Archean to Recent. Geophys. Monogr. Ser., 32: 412–417.

Shackleton, N.J., Berger, A. and Peltier, W.R., 1990. An alternative astronomical calibration of the lower Pleistocene timescale based on ODP Site 677. Trans. R. Soc. Edinburgh, Earth Sci., 81: 251–261.

Sowers, T., Bender, M., Labeyrie, L., Martinson, D., Jouzel, J., Raynaud, D., Pichon, J. and Korotkevich, Y., 1993. A 135,000-year Vostok–Specmap common temporal framework. Paleoceanography, 8: 737–765.

Stax, R. and Stein, R., 1993. Long-term changes in the accumulation of organic carbon in Neogene sediments, Ontong Java Plateau. Proc. ODP, Sci. Results, 130: 573–585.

Stott, L.D., 1992. Higher temperatures and lower oceanic pCO_2: a climate enigma a the end of the Paleocene epoch. Paleoceanography, 7: 395–404.

Takahashi, T., Olafsson, J., Goddard, J.G., Chipman, D.W. and Sutherland, S.C., 1993. Seasonal variation of CO_2 and nutrients in the high-latitude surface oceans: A comparitive study. Global Biogeochem. Cycles 7: 843–877.

Tans, P.P., Fung, I.Y. and Takahashi, T., 1990. Observational constraints on the global atmospheric CO_2 budget. Science, 247: 1431–1438.

Theirstein, H.R., Geitzenauer, K.R., Molfino, B. and Shackleton, N.J., 1977. Global synchroneity of late Quaternary coccolith datum levels: validation by oxygen isotopes. Geology, 5: 400–404.

Van der Burgh, J., Visscher, H., Dilcher, D.L. and Kurschner, W., 1993. Paleoatmospheric signatures in Neogene fossil leaves. Science, 260: 1788–1790.

Washington, W.M. and Meehl, G.A., 1989. Climate sensitivity due to increased CO_2: experiments with a coupled atmosphere and ocean general circulation model. Climate Dynamics, 4: 1–38.

Weiss, R.F., 1974. Carbon dioxide in water and seawater: The solubility of a non-ideal gas. Mar. Chem., 2: 203–215.

Whitman, J.M. and W.H. Berger, 1993. Pliocene–Pleistocene carbon isotope record, Site 586, Ontong Java Plateau. Proc. ODP, Sci. Results, 130: 333–347.

Willebrand, J., 1993. Forcing the ocean with heat and freshwater fluxes. In: E. Raschke (Editor), Energy and Water Cycles in the Climate System. Springer, Berlin, pp. 215–233.

Wilson, A.T. and Long, A., 1993. What was the carbon dioxide content of the glacial atmosphere? Trans. Am. Geophys. Union, 74: 78.